

# *In vitro* effects and *in silico* analysis of newly synthesized pyrrole derivatives on the activity of different isoforms of Cytochrome P450: CYP1A2, CYP2D6 and CYP3A4

Borislav Angelov<sup>1</sup>, Emilio Mateev<sup>2</sup>, Maya Georgieva<sup>2</sup>,  
 Virginia Tzankova<sup>1</sup>, Magdalena Kondeva-Burdina<sup>1</sup>

<sup>1</sup> Faculty of Pharmacy, Medical University – Sofia, Sofia, Bulgaria

<sup>2</sup> Department of Pharmaceutical chemistry, Faculty of Pharmacy, Medical University – Sofia, Sofia, Bulgaria

Corresponding author: Maya Georgieva (maya.bg77@gmail.com)

**Received** 22 October 2022 ♦ **Accepted** 1 November 2022 ♦ **Published** 25 November 2022

**Citation:** Angelov B, Mateev E, Georgieva M, Tzankova V, Kondeva-Burdina M (2022) *In vitro* effects and *in silico* analysis of newly synthesized pyrrole derivatives on the activity of different isoforms of Cytochrome P450: CYP1A2, CYP2D6 and CYP3A4. Pharmacia 69(4): 1013–1017. <https://doi.org/10.3897/pharmacia.69.e96626>

## Abstract

Four pyrrole based hydrazide-hydrazones with established low hepatotoxicity and promising antiproliferative activity were evaluated (at 1 μM concentration) for possible inhibitory activity on human isoforms of Cytochrome P450 CYP1A2, CYP3A4 and CYP2D6. The compounds didn't exert any statistically significant inhibitory effects on CYP1A2 and CYP2D6. However on CYP3A4 only **12** resulted in low statistically significant inhibitory effect decreasing the enzyme activity by 20%, compared to the control (pure CYP3A4). In addition the potential interactions of **12** and the evaluated CYP isoforms were displayed after molecular docking with Glide (Schrödinger). Induced-fit simulations and binding free energy (MM/GBSA) calculations were applied to elucidate the accessibility in each CYP isoform. The most active CYP3A4 inhibitor **12** demonstrated good binding affinity and was in close vicinity to the het Fe ion (2.88 Å). Overall, good correlation between the *in vitro* results and the free binding MM/GBSA recalculations were observed.

## Keywords

CYP450, pyrrole, molecular docking, MM/GBSA

## Introduction

Normally all organisms are constantly exposed on different environmental xenobiotics (natural products or synthetic), which once entered in the body are subjected to elimination through biotransformation processes into non-toxic metabolites. Unfortunately some of these processes may be related to formation of reactive metabolites, with severe toxicity on some targets – cells, tissues or organs. Thus in order to assure the human safety,

it's necessary to have preliminary information about the origin of the toxicant, its mechanism of toxicity and its possible biological interactions.

*In vitro* metabolic investigations are important tool for the drug interactions prediction. Except investigations about enzyme induction and inhibition, it's necessary to have information for the enzymes, responsible for the drug biotransformation (Blaauboer et al. 1994).

The CYP450 superfamily of enzymes consists of more than 55 isoforms, which are involved in the metabolic

pathways of various pharmacologically active compounds. The assessment of CYP450-mediated interactions is of major significance considering the role of the latter enzymes in undesirable drug-drug interactions. Thus, an initial assessment of the CYP450 activity for each active molecule is required in the process of drug development (Iizaka et al. 2021).

Some of the most common representatives of CYP450 family are CYP1A2, CYP2D6, CYP3A4. Among them CYP1A2 is localized to the endoplasmic reticulum and its expression is induced by molecules containing aromatic hydrocarbon chain, along with some natural products like caffeine, aflatoxin B1 and some drugs, like paracetamol (Matetzky et al. 2004; Bliden et al. 2008). Another representative of CYP450 family is CYP2D6. This isoform is primarily expressed in the liver and highly expressed in areas of the central nervous system, including the *substantia nigra*. In particular this enzyme is related to the metabolic transformations and elimination of approximately 25% of clinically used drugs (Wang et al. 2009). It is also responsible for activation of some prodrugs (Wang et al. 2014).

Cytochrome P450 enzymes are essential for the metabolism of many medicines and endogenous compounds. The CYP3A family is the most abundant subfamily of the CYP isoforms in the liver. There are at least four isoforms: 3A4, 3A5, 3A7 and 3A43 of which 3A4 is the most important (Ince et al. 2013). This isoform contributes to bile acid detoxification, termination of action of steroid hormones, and elimination of phytochemicals in food and the majority of medicines (Kacevska et al. 2008; Zanger and Schwab 2013). In general this enzyme is subjected to reversible and irreversible inhibition which is a reason for its inactivation (Zhou 2008).

Recently, the reliability and robustness of the *in silico* methods for the assessment of CYP450 activities has increased substantially. Studies based on the implementation of web servers (Ekroos and Sjogren 2006) and molecular docking simulations (Chand et al. 2021) have displayed good correlation with the *in vitro* results.

Consequently, the aim of the current work was to investigate the inhibition potency of four potent pyrrole-based compounds on human CYP1A2, CYP2D6, and CYP3A4 enzymes through *in silico* and *in vitro* studies. Molecular docking simulations demonstrated the possible conformations of the title compounds in the active sites of the three isoforms. Furthermore, induced-fit docking (IFD) and MM/GBSA free energy recalculations were introduced to enhance the fidelity of the *in silico* results.

## Materials and methods

### *In vitro* assay

The potential inhibitory activity of the compounds **11**, **11I**, **12** and **12a** on the evaluated Cytochrome P450 enzyme isoforms was measured using the corresponding specific fluorimetric screening kits CYP1A2 Inhibitor Screening Kit (Fluorometric) (Abcam) with 3-cyano-7-hydroxycoumarin (3-CHC) applied as substrate and  $\alpha$ -naphthoflavone used as an

inhibitor. The CYP2D6 Inhibitor Screening Kit (Fluorometric) (Abcam) with 3-[2-(N,N-diethyl-N-methylammonium ethyl)-7-methoxy-4-methylcoumarin applied as a substrate and quinidine as an inhibitor, and CYP3A4 Inhibitor Screening Kit (Fluorometric) (Abcam) with resorufin applied as a substrate and ketoconazole as an inhibitor. The fluorescence for the different isoforms was measured at Ex/Em = 406/468 nm for CYP1A2; Ex/Em = 535/587 nm for CYP3A4 and Ex/Em = 390/468 nm for CYP2D6, respectively.

### Statistical analysis

The different CYP450 isoform activity were normalized as percentage of the untreated control set as 100% and the results were expressed as mean values and standard deviation ( $\pm$ SD) (Graph Pad Prism). Statistical analysis was performed by one-way analysis of variance (ANOVA) with post hoc multiple comparisons procedure (Dunnett's test) to assess the statistical differences in case of normal distribution. Values of  $p < 0.05$  and  $p < 0.001$  were considered statistically significant.

### Molecular docking

#### Selection and preparation of proteins

The crystallographic structures of the employed in this study CYP isoforms – CYP1A2 (PDB ID: **2HI4**) (Marchal et al. 2006), CYP2D6 (PDB ID: **4WNU**) (Olsen et al. 2015) and CYP3A4 (PDB ID: **2V0M**) (Pang et al. 2018), resolved with the co-crystallized ligands  $\alpha$ -naphthoflavone, quinidine and ketoconazole, respectively, were retrieved from the Protein Data Bank (PDB). The Protein Preparation module in Maestro (Schrödinger Release 2021-3: Protein Preparation Wizard; Epik, Schrödinger, LLC, New York, NY, 2021.) was employed for the protein refinements. Hydrogen bonds and het states at pH 7.0  $\pm$  2.0 were produced followed by the removal of non-active water molecules. Subsequently, the energies of the crystallographic structures were minimized with the OPLS2005 force field. The grid box was generated around each co-crystallized ligand with the Receptor Grid Generation module in Maestro.

#### Ligands preparation

The chemical structures of the title compounds were drawn in the 2D sketcher module of Maestro, and converted to the corresponding 3D structures with Ligprep (Schrödinger Release 2021-3: LigPrep, Schrödinger, LLC, New York, NY, 2021.). Utilizing the latter module, hydrogen bonds, tautomers, and ionization states at pH 7.0  $\pm$  2.0 were obtained. The charged groups were neutralized. Furthermore, the ligands' energies were minimized with the OPLS2005 force field.

#### Docking protocol

The molecular docking was carried out with the licensed software Glide (Schrödinger Release 2021-3: Glide, Schrödinger, LLC, New York, NY, 2021.). The former

implements an empirically based scoring algorithm, which includes three options: High-throughput screening (HTS), Standard-Precision (SP) and Extra-Precision (XP) modes. For the current study the most precise docking mode – XP, was utilized. To further explore the obtained active conformations, the Induced-fit docking (IFD) mode in Maestro was employed. The IFD examines the protein's side chains as fully flexible, which leads to exhaustive sampling. Finally, MM/GBSA (Molecular Mechanics-Generalized Born Surface Area) recalculations were introduced to determine the binding free energies of the acquired complexes.

## Results and discussion

### Selection of the target compounds

Preliminary evaluations of hepatotoxicity and antiproliferative activity of two series of synthesized by us pyrrole-based hydrazone-hydrazones were recently published (Georgieva et al 2022) and outlined four representatives with low toxic effects and promising activity, identified as **11**, **11I**, **12** and **12a**. The structures of the evaluated compounds is presented on Fig. 1.

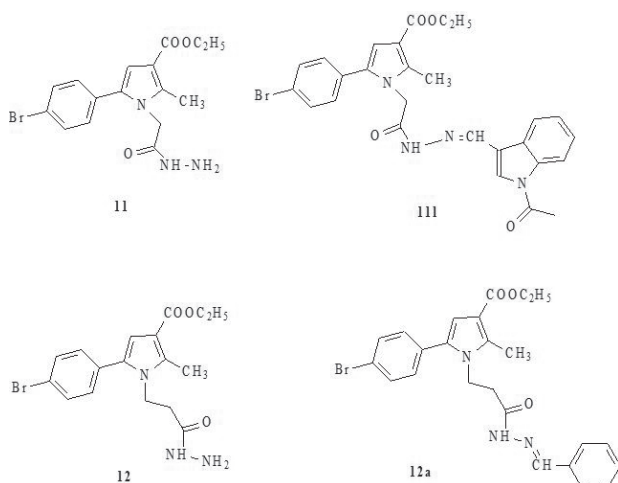


**Figure 1.** Structures of target evaluated compounds.

### In vitro evaluations

The evaluated compounds **11**, **11I**, **12** and **12a** were tested for possible inhibitory activity on some human isoforms of Cytochrome P450 at concentration 1  $\mu$ M. Three enzymes were chosen: the localized to the endoplasmic reticulum CYP1A2, the primarily expressed in the liver and highly expressed in areas of central nervous system (CNS) CYP2D6 and the available in the liver and in the intestine CYP3A4.

The target compounds were tested as CYP1A2 and CYP2D6 potential inhibitors. The results from the performed evaluations are presented on Figs 2, 3, respectively.

The results indicated that the compounds didn't show any statistically significant inhibitory effects on CYP1A2 and CYP2D6 (Figs 2, 3).

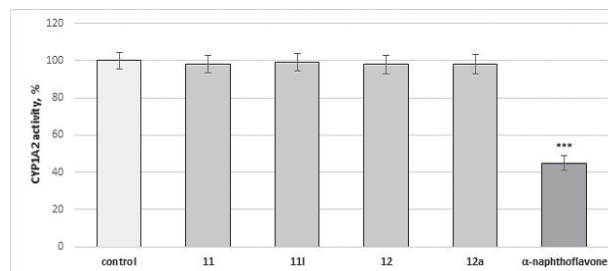


**Figure 2.** Effects of compounds **11**, **11I**, **12** and **12a** (at concentration 1  $\mu$ M) on the CYP1A2 enzyme activity. \*\*\*  $P < 0.001$  vs control (pure CYP1A2).

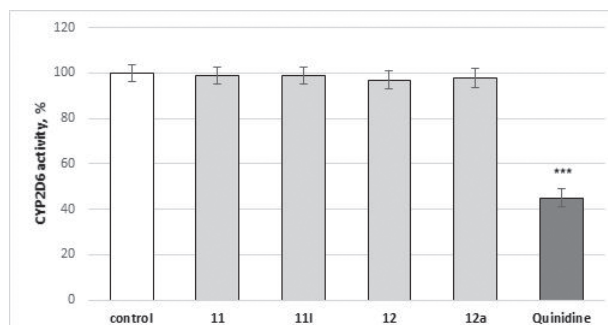


**Figure 3.** Effects of compounds **11**, **11I**, **12** and **12a** (at concentration 1  $\mu$ M) on the CYP2D6 enzyme activity. \*\*\*  $P < 0.001$  vs control (pure CYP2D6).

In addition all evaluated structures were analyzed for potential inhibitory effects on CYP3A4, and the results are presented on Fig. 4.

The observations identified that only compound **12** shows low statistically significant inhibitory effect by decreasing the enzyme activity by 20%, compared to the control (pure CYP3A4). The other 3 tested derivatives didn't reveal any effects on the CYP3A4 enzymatic activity (Fig. 4).

The effects on each isoform of Cytochrome P450 were compared with the relevant enzyme inhibitor. For CYP1A2 is  $\alpha$ -naphthoflavone, for CYP2D6 is quinidine and CYP3A4 is ketoconazole. These inhibitors decreased statistically significant the enzyme activity by 55%, compared to the control (pure enzyme) (Figs 2–4).

The performed analysis identified the evaluated compounds as poor inhibitors to the discussed CYP's, with **12** performing highest inhibitory activity among others, but

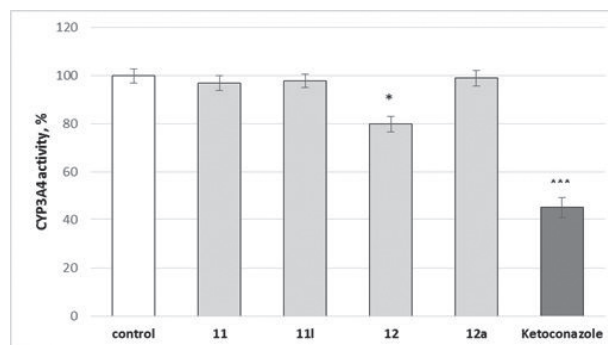


**Figure 4.** Effects of compounds **11**, **11I**, **12** and **12a** (at concentration 1  $\mu$ M) on the CYP3A4 enzyme activity. \*  $P < 0.05$ ; \*\*\*  $P < 0.001$  vs control (pure CYP3A4).

still lower than the applied comparative agents. This results are a prerequisite to consider all of the evaluated compounds as substances with low effect of hepatic metabolism and decreased possibility for drug-drug interactions performance.

## Re-docking simulations

The docking module of Maestro – Glide was implemented for the current study considering the recent success rate when CYP enzymes were applied in the docking with the latter software (Ridhwan et al. 2022). Initially, self-docking simulations were carried out to assess the reliability of the docking software to correctly generate the conformations of the co-crystallized ligands back into the active sites of CYP1A2 (PDB:2HI4), CYP2D6 (PDB:4WNU) and CYP3A4 (PDB:2V0M). The Extra-Precision docking led to root mean square deviation (RMSD) values under 1 Å in all crystallographic structures. Thus, the Glide's docking protocols demonstrate reliable results when CYP1A2, CYP2D6 and CYP3A4 are employed.

## Molecular docking simulations

After the validation of the crystallographic structures, all four ligands were docked into the three CYP isoforms to observe the potential correlation between the *in vitro* and the *in silico* results, and also to discuss the active conformation of the active CYP3A4 inhibitor – **12**. The data from the docking simulations is provided in Table 1. The co-crystallized ligands were docked in their native enzymes for reference.

In the active site of CYP1A2 (PDB: 2HI4) only **11** and **12** demonstrated moderate binding affinities of -7.80 and -8.21, respectively. After employing the more exhausting search in the active site with the IFD, the binding energies dropped to -5.57 and -6.36. The binding free energies calculated with the MM/GBSA were drastically lower compared to the value of the co-crystallized ligand. Subsequent docking in the CYP2D6 isoform agreed with the experimental

data. In the latter case **11** and **12** showed the best results, however their binding scores were negligible compared to the scores of the native CYP2D6 inhibitor quinidine.

Interestingly, the results from the simulations in the active site of CYP3A4 demonstrated similar results for all four ligands. When the Extra-precision option in Glide was applied, the binding affinities were in the range of -6.57 to -8.28. In comparison, the co-crystallized ligand – ketoconazole, displayed XP score of -10.14. After the additional recalculations with IFD and MM/GBSA the most prominent results were demonstrated by compounds **12** and **12a**. However, the key difference between the two conformations was the distance between the het group and the ligands. In the case of **12a** the distance was calculated to be 5.64 Å while **12** was in close vicinity to the het structure (2.88 Å). The length between the heme Fe ion and the observed ligand could be used as a criterion to determine the robustness of the binding orientation. Typically, a pose is considered as reliable if the distance is shorter than 6 Å (Bonomo et al. 2017).

To further observe the intermolecular interactions of the complex **12-2V0M**, both the 2D and 3D visualizations are presented (Fig. 5).

Based on the visualized stabilization forces, the hem group and Phe304 were the major drug-binding residues in CYP3A4. The latter formed strong p-p bonds with the pyrrole ring and the benzene moiety. Several weak hydrophobic interactions were formed by the active amino residues Ile120, Leu210, Leu211, Phe241, Ala305, Ile369, Leu482 and Leu483. After the XP docking, the active pose of **12** demonstrated that the carbonyl group from the ester group was in close proximity to the hem structure. In contrast, the more hardware demanding, and more precise IFD displayed different orientation in the active site of CYP3A4. During the latter simulations the hydrazide-hydrazone moiety was facing the hem moiety. Therefore, the implementation of IFD for virtual simulations in various CYPs isoforms is essential considering the enhanced reliability of the acquired results (Ridhwan et al. 2022).

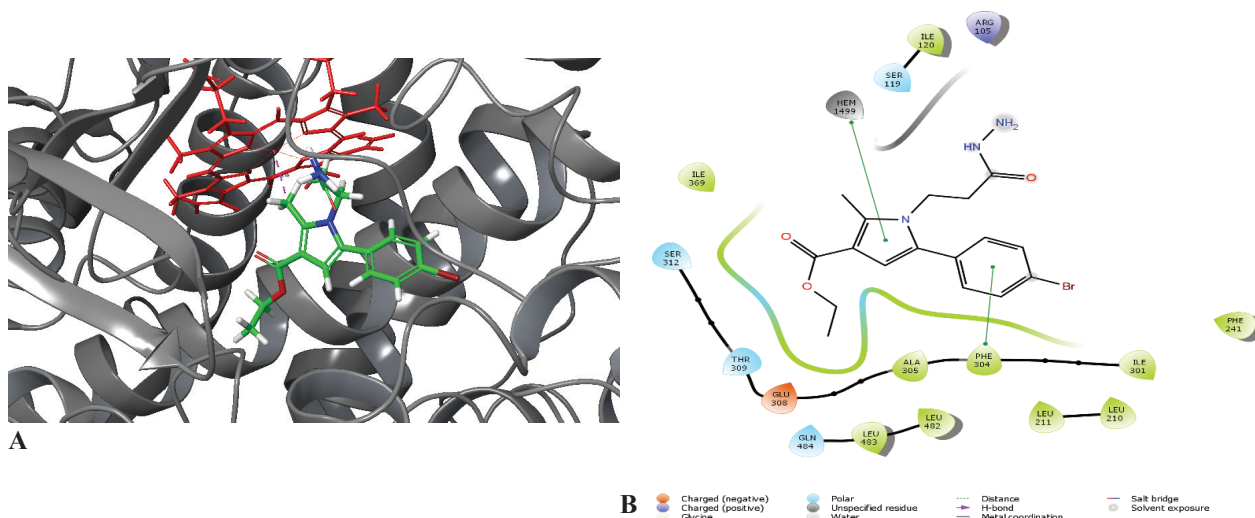


**Figure 5.** Visualized major intermolecular interactions of the pyrrole-based compound **12** in the active site CYP3A4 (PDB: 2V0M) after employing IFD and MM/GBSA recalculations. The interactions are provided in both 3D (A) and 2D (B) forms. The enzyme is depicted in grey, the hem group is given in red, and the active inhibitor – **12**, is presented as green sticks.

**Table 1.** Binding energies of the title ligands with human CYP1A2, CYP2D6 and CYP3A4.

Compound	CYP1A2			CYP2D6			CYP3A4		
	XP Glide	IFD	MM/GBSA	XP Glide	IFD	MM/GBSA	XP Glide	IFD	MM/GBSA
11	-7.80	-5.57	-43.53	-5.44	-5.83	-31.91	-6.75	-5.31	-59.41
111	n.r.	n.r.	n.r.	n.r.	n.r.	n.r.	-6.57	-6.84	-63.33
12	-8.21	-6.36	-54.22	-4.43	-5.21	-22.00	-7.77	-7.99	-79.13
<b>12a</b>	<b>n.r.</b>	<b>n.r.</b>	<b>n.r.</b>	<b>n.r.</b>	<b>n.r.</b>	<b>n.r.</b>	<b>-8.28</b>	<b>-10.3</b>	<b>-86.24</b>
alpha-naphthoflavone	-10.82	-11.24	-89.435	n.d.	n.d.	n.d.	n.d.	n.d.	n.d.
quinidine	n.d.	n.d.	n.d.	-9.89	-10.29	-101.9	n.d.	n.d.	n.d.
ketoconazole	n.d.	n.d.	n.d.	n.d.	n.d.	n.d.	-10.14	-11.43	-117.64

\*n.d.: not determined; n.r.: no result.

## Conclusion

In conclusion, none of the evaluated compounds didn't exert any statistically significant inhibitory effects on CYP1A2 and CYP2D6. However on CYP3A4 only **12** resulted in low statistically significant inhibitory effect decreasing the enzyme activity by 20%, compared to the control (pure CYP3A4). The *in silico* and *in vitro* data

demonstrated that the pyrrole-based compound **12** is a weak CYP3A4 inhibitor with no effects against CYP1A2 and CYP2D6. The results should be examined as a source of future unwanted drug-drug interactions. Furthermore, the docking simulations demonstrated that the initial IFD followed by free binding energy recalculation with MM/GBSA provided highly reliable conformations compared to other searching and scoring algorithms.

## References

- Blauboer J, Boobis AR, Castell JV, Coecke S, Groothuis GMM, Guilouzo A, Wiebel FJ (1994) The practical applicability of hepatocyte cultures in routine testing. *Alternatives to Laboratory Animals* 22(4): 231–241. <https://doi.org/10.1177/026119299402200404>
- Bliden K, Dichiaro J, Lawal L, Singla A, Antonino M, Baker B, Bailey W, Tantry U, Gurbel P (2008) The association of cigarette smoking with enhanced platelet inhibition by clopidogrel. *Journal of the American College of Cardiology* 52: 531–533. <https://doi.org/10.1016/j.jacc.2008.04.045>
- Bonomo S, Jørgensen FS, Olsen L (2017) Dissecting the Cytochrome P450 1A2- and 3A4-Mediated Metabolism of Aflatoxin B1 in Ligand and Protein Contributions. *Chemistry – A European Journal* 23(12): 2884–2893. <https://doi.org/10.1002/chem.201605094>
- Chand RR, Nimick M, Cridge B, Rosengren RJ (2021) In vitro hepatic assessment of cineole and its derivatives in common brushtail possums (*Trichosurus vulpecula*) and Rodents. *Biology* 10(12): 1326. <https://doi.org/10.3390/biology10121326>
- Ekroos M, Sjogren T (2007) Structural basis for ligand promiscuity in cytochrome P450 3A4. *Proceedings of the National Academy of Sciences* 103(37): 13682–13687. <https://doi.org/10.1073/pnas.0603236103>
- Iizaka Y, Sherman DH, Anzai Y (2021) An overview of the cytochrome P450 enzymes that catalyze the same-site multistep oxidation reactions in biotechnologically relevant selected actinomycete strains. *Applied Microbiology and Biotechnology* 105(7): 2647–2661. <https://doi.org/10.1007/s00253-021-11216-y>
- Ince I, Knibbe CAJ, Danhof M, de Wildt SN (2013) Developmental changes in the expression and function of Cytochrome P450 3A Isoforms: Evidence from in vitro and in vivo investigations. *Clinical Pharmacokinetics* 52: 333–345. <https://doi.org/10.1007/s40262-013-0041-1>
- Kacevska M, Robertson GR, Clarke SJ, Liddle C (2008) Inflammation and CYP3A4-mediated drug metabolism in advanced cancer: impact and implications for chemotherapeutic drug dosing. *Expert Opinion on Drug Metabolism and Toxicology* 4: 137–149. <https://doi.org/10.1517/17425255.4.2.137>
- Marechal JD, Yu J, Brown S, Kapelioukh I, Rankin EM, Wolf CR, Sutcliffe MJ (2006) In silico and in vitro screening for inhibition of cytochrome p450 cyp3a4 by comedication commonly used by patients with cancer. *Drug Metabolism and Disposition* 34(4): 534–538. <https://doi.org/10.1124/dmd.105.007625>
- Matetzky S, Shenkman B, Guetta V (2004) Clopidogrel resistance is associated with increased risk of recurrent atherothrombotic events in patients with acute myocardial infarction. *ACC Current Journal Review* 13: 9. <https://doi.org/10.1016/j.accreview.2004.08.004>
- Pang X, Zhang B, Mu G, Xia J, Xiang Q, Zhao X, Cui Y (2018) Screening of cytochrome P450 3A4 inhibitors via in silico and in vitro approaches. *RSC advances* 8(61): 34783–34792. <https://doi.org/10.1039/C8RA06311G>
- Ridhwan MJM, Bakar SIA, Latip NA, Ghani NA, Ismail NH (2022) A comprehensive analysis of human CYP3A4 crystal structures as a potential tool for molecular docking-based site of metabolism and enzyme inhibition studies. *Journal of Computational Biophysics and Chemistry* 21(03): 259–285. <https://doi.org/10.1142/S2737416522300012>
- Wang A, Stout D, Zhang Q, Johnson E (2015) Contributions of ionic interactions and protein dynamics to cytochrome P450 2D6 (CYP2D6) substrate and inhibitor binding. *Journal of Biological Chemistry* 290(8): 5092–5104. <https://doi.org/10.1074/jbc.M114.627661>
- Wang B, Yang L-P, Zhang X-Z, Huang S-Q, Bartlam M, Zhou S-F (2009) New insights into the structural characteristics and functional relevance of the human cytochrome P450 2D6 enzyme. *Drug Metabolism Reviews* 41: 573–643. <https://doi.org/10.1080/03602530903118729>
- Wang X, Li J, Dong G, Yue J (2014) The endogenous substrates of brain CYP2D. *European Journal of Pharmacology* 724: 211–218. <https://doi.org/10.1016/j.ejphar.2013.12.025>
- Zhou SF (2008) Potential Strategies for Minimizing Mechanism-Based Inhibition of Cytochrome P450 3A4. *Current Pharmaceutical Design* 14: 990–1000. <https://doi.org/10.2174/138161208784139738>